XIVth Congress of the International Society for Photogrammetry
Hamburg 1980

Commission III
Presented Paper

INTERNAL RELIABILITY MODELS FOR AERIAL BUNDLE SYSTEMS

Armin Grün

Chair for Photogrammetry
Technical University Munich
Arcisstr. 21
8 München 2, West Germany

Presently:
Department of Geodetic Science
The Ohio State University
1958 Neil Avenue
Columbus, Ohio 43210
U.S.A.

Summary: The reliability of a photogrammetric system defines its quality with respect to gross error detection and location. The elements of the Q_{VV}-matrix are crucial for the internal reliability. A sophisticated blunder test procedure is available with the "data-snooping" technique, which requires the diagonal elements of Q_{VV}.

For large linear systems, as they usually appear in aerial triangulation the computation of the complete Q_{VV}-matrix or even of its diagonal elements (q_{VV}) only becomes very costly. So it is useful to apply approximate diagonal elements of Q_{VV}, which can be obtained from reliability models.

These models are developed and the main parameters which influence the q_{VV}-values are investigated.

Factors to be considered early in the stage of project planning, if a highly reliable photogrammetric system is required, are indicated as an important by-product.

Internal Reliability Models for Aerial Bundle Systems

1. Introduction

In a previous paper (Grün (2)) a concept for gross error detection in bundle adjustment was presented, which is now realized in the bundle program MBOP (Chair for Photogrammetry, Technical University, Munich). This concept contains two stages of blunder detection. The check on larger gross errors, which are mostly due to errors in interpretation and numbering, is performed simultaneously with the computation of initial values for bundle adjustment (checking in several stages: model formation, strip formation, strip orientation).
This inexpensive process guarantees a cleaner data set before bundle adjustment is started. The residuals at image coordinates of bundle adjustment are then subject to a modified data-snooping test procedure.
The application of strict methods for blunder detection in aerial photogrammetric systems, as Baarda's data-snooping (Baarda (1)), is not to be recommended for general use, since the computation of all diagonal elements of the Q_{vv}-matrix causes an enormous computational amount even in medium size systems. In fact the strict computation of all q_{vv}-values is not necessary, as is explained later.
Aerial photogrammetric systems have usually a very regular network structure. This fact can be exploited to use q_{vv}-values derived from internal reliability models instead of strictly computed values. This idea is reinforced by an essential feature of the q_{vv}-values. They are mainly dependent on parameters which are easy to establish in a practical project: i.e. the local redundancy, the number of image points per photo and the type of ground point (control or non-control). Whereas in Grün (2) a real practical block has been used to investigate the main parameters influencing the internal reliability, this paper presents more comprehensive internal reliability models based on synthetic data. The development of these models pursues two main purposes. On the one hand, they can be applied to obtain approximate standard deviations for the residuals to be used in a modified data-snooping procedure and on the other, they provide for deeper insights into reliability structures of bundle systems thus leading to the knowledge necessary for avoiding unreliable systems early in the stage of project planning.

2. Modified data-snooping test procedure

Baarda proposes to apply his data-snooping procedure after the test criterion $\frac{\hat{\sigma}_o^2}{\sigma_o^2}$ has indicated blunders in the data (Baarda (1)). This global test, however, is too global a measure for photogrammetric blocks to be used as a basis for deciding whether the data-snooping should be applied. If the data set contains only a few small gross errors, they can easily be absorbed within the global measure and thus do not show up in the global test, although they perhaps could be detected by the data-snooping tests (by testing the individual residuals). Additionally, the uncertainty concerning the expectation σ_o is too big to use σ_o for making such a far reaching decision. So it is suggested to apply the data-snooping test in any case, no matter what result a global test would show, as the probability is almost 100% that a practical photogrammetric block has at least one small blunder left to be detected by data-snooping.
The original data-snooping procedure consists in the testing of a sequence of null hypotheses

$$H_{o_i}: \; E(v_i) = 0 \qquad i = 1,..,n \qquad (1)$$

n = number of observations

by using the test criterions

$$w_i = \frac{-v_i}{\sigma_{v_i}}\ , \qquad \sigma_{v_i} = \sigma_o \sqrt{q_{v_i v_i}} \tag{2}$$

If H_{o_i} is true, then w_i is distributed as Student's t :

$$w_i \sim t(1-\alpha_o,\infty)\ , \qquad \alpha_o \ldots \text{type I error size} \qquad \alpha_o = P(|w_i| > t(1-\alpha_o,\infty)/H_{o_i}) \tag{3}$$

The data-snooping is - besides Pope's (3) procedure - the most sensitive of all known blunder detection techniques. Each individual residual is compared with its own standard deviation, thus taking into account the design matrix A of the network. In addition, this theory can be extended to cover adjacent problems, viz.:

- the alternative hypothesis concept, which opens the possibility of indicating the maximal size of a just non-detectable blunder (internal reliability indication)
- the external reliability concept, which enables the computation of the effect of a just non-detectable blunder on to the object space coordinates of ground points or their functions.

Of crucial importance in all reliability considerations are the q_{vv}-values, the diagonal elements of Q_{vv}.

Q_{vv} is given by $$Q_{vv} = P^{-1} - A(A^TPA)^{-1}A^T\ , \tag{4}$$
which indicates the tremendous amount of computation necessary for Q_{vv} for medium or large bundle systems.

The theoretical foundation of data-snooping is based on the restriction that only one gross error appears in the observation set. Since this can never be assumed to be true in practice, the efficiency of data-snooping is determined by the structure of Q_{vv}. The residuals of adjustment can be represented by

$$v = -Q_{vv}P\ell\ ; \qquad \ell \ldots \text{observation vector} \tag{5}$$

Hence, a gross error vector $\nabla\ell$ is transformed as

$$\nabla v = -Q_{vv}P\nabla\ell \tag{6}$$

Diagonal dominance of Q_{vv} means that a blunder in the ith observation $\nabla\ell_i$ shows mainly up in the related residual v_i as ∇v_i (compare (6)).

Hence diagonal dominance of Q_{vv} is equivalent to good blunder location property of the system. As far as bundle systems are concerned, good location property again is equivalent to good detection property (the detection property is determined by the size of the diagonal elements of Q_{vv}). That means, the efficiency of data-snooping is strongly dependent on the reliability of the system.

Considering in addition the uncertainty in the assumption of the weight matrix P it turns out to be unnecessary to compute strictly all q_{vv}-values even for medium and large size blocks.

Therefore a modified data-snooping procedure is suggested.

- Suppose approximate values $\sqrt{q_{vv}}^{\,o}$ for $\sqrt{q_{vv}}$ are available with a tolerance of $\pm\, k_q\%$:

$$k_q = \frac{(\sqrt{q_{vv}} - \sqrt{q_{vv}}^{\,o}) \cdot 100}{\sqrt{q_{vv}}^{\,o}} \tag{7}$$

- Compute for all observations approximate test criterions $w_i^{\,o}$ by using $\sqrt{q_{v_iv_i}}^{\,o}$:

$$w_i^{\,o} = \frac{-v_i}{\hat{\sigma}_{v_i}^{\,o}}\ , \qquad \hat{\sigma}_{v_i}^{\,o} = \hat{\sigma}_o \sqrt{q_{v_iv_i}}^{\,o} \tag{8}$$

- Reject all observations which lead to

$$|v_i| > c\left(1 + \frac{k_q}{100}\right)\hat{\sigma}_{v_i}^{\,o} \tag{9}$$

(c = critical value of rejection from t-distribution)

- Accept all observations which lead to

$$|v_i| < c(1 - \frac{k_q}{100})\hat{\sigma}_{vi}{}^{o} \tag{10}$$

- Compute the exact q_{vv}-values only for those observations which lead to

$$c(1 - \frac{k_q}{100})\hat{\sigma}_{vi}{}^{o} \le |v_i| \le c(1 + \frac{k_q}{100})\hat{\sigma}_{vi}{}^{o} \tag{11}$$

This procedure reduces the computational amount considerably, as only a small part of all q_{vv}-values has to be computed explicitly. On the other hand, it requires an algorithm which is able to pick out individual q_{vv}-values with a minimum of computational expense. Such an algorithm, which fits easily into existing bundle programs, is given by the following derivation. Suppose a column vector of the identity matrix

$$f_i{}^T = (0,\ldots 0,1,0,\ldots 0) \ . \tag{12}$$

Regard f_i as observation vector and compute the related solution vector

$$x_i = (A^TPA)^{-1} A^TPf_i \ . \tag{13}$$

If Q_{vv} ($Q_{vv} = P^{-1} - A(A^TPA)^{-1}A^T$) is multiplied from the right by Pf_i then one gets

$$Q_{vv}Pf_i = If_i - A(A^TPA)^{-1}A^TPf_i \tag{14}$$

and with (13)

$$Q_{vv}Pf_i = f_i - Ax_i \tag{15}$$

If P is diagonal, equation (15) indicates a fast and easy way to compute the desired elements of Q_{vv}.
Let $f_i{}^T$, P and Q_{vv} be

$$f_i{}^T = (1,0,\ldots,0) \ ,$$

$$P = \begin{pmatrix} p_1 & & 0 \\ & p_2 & \\ 0 & & \ddots\ p_n \end{pmatrix} , \qquad Q_{vv} = \begin{pmatrix} q_{11} & \cdots & q_{1n} \\ \vdots & & \vdots \\ q_{n1} & \cdots & q_{nn} \end{pmatrix} \tag{16}$$

and a_i the ith row of A.
Then holds

$$q_{11} = \frac{1 - a_1x_1}{p_1} \ , \qquad q_{21} = \frac{0 - a_2x_1}{p_1} \ ,\ldots\ldots, \qquad q_{n1} = \frac{0 - a_nx_1}{p_1} \ ,$$

or more generally

$$q_{ki} = \frac{t - a_kx_i}{p_i} \ , \qquad \text{with } t = \begin{cases} 1 \text{ if } k = i \\ 0 \text{ if } k \ne i \end{cases} \tag{17}$$

So for each vector f_i which leads to the ith column of Q_{vv} one needs as essential operations only the reduction of the right hand side of the system of normal equations and the back substitution to obtain x_i.

The kernels of the data-snooping procedure are the q_{vv}-values, which are responsible for the quality of the internal reliability of a system. In a previous investigation (Grün (2)), two main parameters influencing the amount of q_{vv} have been indicated. In the following chapter a more comprehensive investigation is presented based on synthetic data and including the formulation of interior reliability models to be used for the modified data-snooping procedure.

3. Derivation of internal reliability models

The individual internal reliability values of a system are usually given by the amount of a just non-detectable gross error $\nabla \ell_i$ (weight matrix P of the observations assumed to be diagonal):

$$\nabla \ell_i = \frac{\delta \cdot \sigma_o}{\sqrt{q_{v_i v_i}} \cdot p_i} \qquad (18)$$

δ... non-centrality parameter for the data-snooping test
p_i... weight of the ith observation

This is a proper formulation for use in a special project, but it is not suitable for general reliability models, as in this case one should apply standardized values to be independent of σ_o and the non-centrality parameter δ. Hence in this investigation the $\sqrt{q_{v_i v_i}}$-values are used as internal reliability measures, which reflect the network structure and are independent of σ_o and the chosen probability levels.
The material for this investigation was selected according to the experiences gained in Grün (2). All computations are based on synthetic data.

Data specifications:
- Camera constant c = 150 mm
- Flat terrain; equal flying height; $\phi = \omega = \kappa = 0$
- Two sets of regular image point distributions:
  3x3=9 and 5x5-25 points per photograph
- 60% forward overlap, 60% sidelap
- Two blocks of different sizes: 4x4=16 photographs, 7x7=49 photographs
- 3 different control distributions in each block (see Figure 1); every control distribution is investigated twice: normal version and "twin control" version ("twin control" $\hat{=}$ pairs of control, points close together)
- Image coordinates uncorrelated and of equal precision (p_i=1)
- Control assumed to be free of errors

The computation of the individual q_{vv}-values has been performed according to the method of "identity matrix observation" as described in the section 2; it is based on strict block adjustments.
In Grün (2) the computations had been founded on the assumption of measurements made in the monocomparator mode, i.e. each image point is observed only once. The advantages of stereocomparator measurements are sufficiently well-known and most of the measurements in practice are stereomeasurements. So the investigations presented in this paper are based on stereomode simulations, i.e. all image points of adjacent models within a strip are supposed to be measured twice, thus leading to two sets of image coordinate observations ("twin rays").

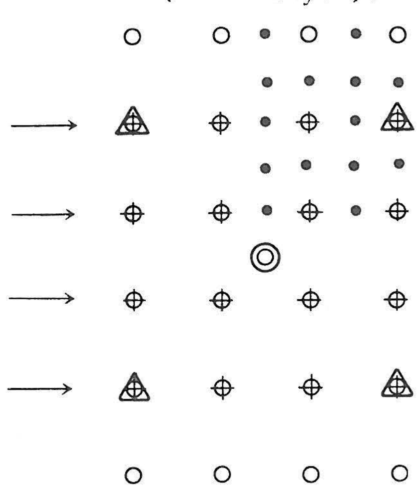

+ ...nadir points
○...ground points according to 3x3 image point distribution (one additional point in the block center)
●...additional ground points according to 5x5 image point distribution (only a part of all block points are plotted)
△ ○ ...locations of control points for i=3b
⟶ ...assumed flight strips

Figure 1a: Distributions of ground points and camera locations for the 4x4 photo block

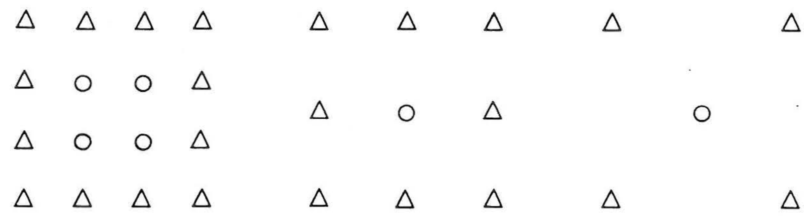

4x4 photo block:	i=1b	i=1.5b	i=3b
7x7 photo block:	i=2b	i=3b	i=6b

Figure 1b: Control distributions

i = bridging distance
b = base unit

Table 1: Computation versions
(per version: single control and twin control)

Block Size (photos)	Image Point Distribution	Control Distribution i=1b	i=1.5b	i=2b	i=3b	i=6b
4x4	3x3 5x5	43 45	43 45	-- --	43 45	-- --
7x7	3x3 5x5	-- --	-- --	73 75	73 75	73 75

Figure 2 shows the ray configurations considered in these investigations. Only "complete" ray configurations - implying observation sets made in stereomode measuring process and no observation neglected - have been used. Other possible configurations have not been utilized.

o ...projection center
O ...non-control point
Δ ...control point
I ..."inner" ray (double observation)
O Δ ...ray configuration to be found at non-control and control points

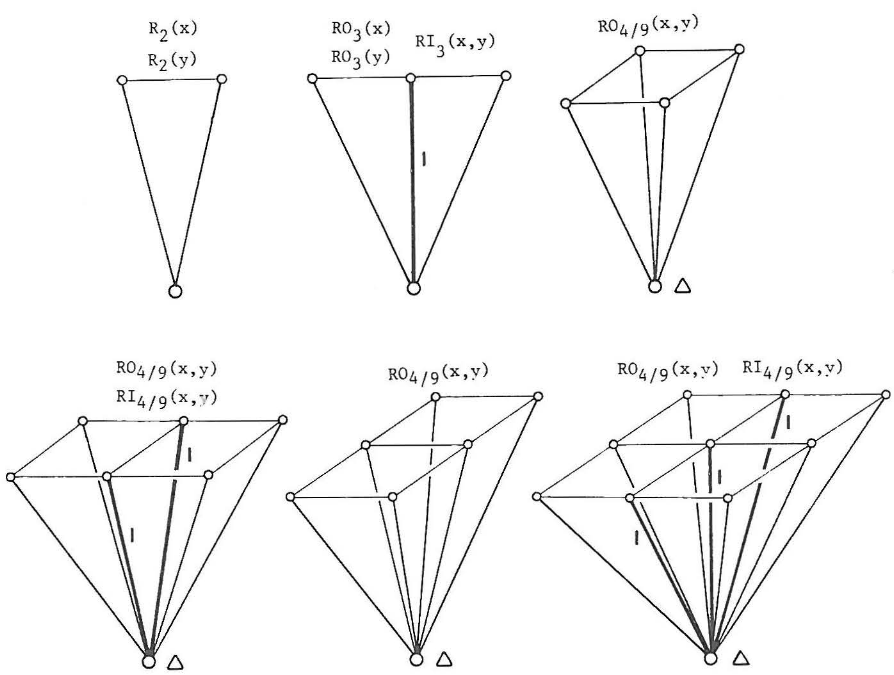

Figure 2: Ray configurations used in the blocks investigated ("complete" ray sets)

According to the experiences gained with the investigations in Grün (2) the ground points have been partitioned into classes which depend on the number of rays intersecting at that point and on the point characteristic (control or non-control point). The point classifications can be seen from Figure 2. As an example, the classification symbol "RO3(y)" has to be read as "average $\sqrt{q_{vv}}$-value for y-residuals of outer rays of points with 3 rays", and "RI4/9 (x,y)" as "average $\sqrt{q_{vv}}$-value for x- and y-residuals of inner rays of points with 4 to 9 rays". Points with 4 to 9 rays have been collected in only one class since a 4-ray point has almost the same reliability values as a 9-ray point (see Grün (2)).
To get an identical counting and classification technique for mono mode and stereo mode observations, the counting of rays has been performed by counting the twin rays (double observations) as one ray only. The distinction between twin rays and single rays is made by introducing separate classes (i.e. separate average $\sqrt{q_{vv}}$-values) for the twin rays. These are denoted by the letter I ("inner" rays).
Figures 3-8 show the internal reliability models obtained with the data used here. To investigate a possible dependence on the bridging distance (i), this parameter is introduced as one axis. The other axis represents average $\sqrt{q_{vv}}$-values denoted as "point means" ($\sqrt{q}^{\,p}$). These are the means of the $\sqrt{q_{vv}}$-values of all observations of all points belonging to the indicated class.
Starting with the analysis of the non-control point observations, one notices (see Figures 3 and 4) that there is no real dependence on the bridging distance. The inner rays RI show throughout a significant better reliability than the outer rays RO. While these inner ray values are fairly resistant to a change in image point distribution (3x3 against 5x5) this is not true for the outer ray values. Extraordinarily large differences show up in Figure 4 for the R2(y) - and the RO3(y) - values comparing the 3x3 and the 5x5 image point versions. This is due to the fact that in the data used, R2-observations appear only in the corner models of the block and RO3-observations only in the edge models of the block. In the 3x3 image point versions, the corner photos possess only 6 image points (only half the photo is covered) thus leading to worse reliability values all around.
This effect becomes quite obvious if the small block (4x4 photos) and the large block (7x7 photos) versions for RO3(y) are compared. Within the small block version, each 3-ray point has one ray from a corner photo, which causes the average values to deteriorate.
The analysis of the control points shows (Figure 5) that the outer ray values are slightly dependent on the bridging distance, whereas the inner ray values are fairly constant. Again the outer ray values are more sensitive to a change in the number of image points.
The definition of "good" internal reliability is relative, of course. If $\sqrt{q_{vv}}$-values of about 0.5 are already regarded as being of sufficient reliability, then the RO3(x)-values and the R2(y)-values of the 3x3 image point distribution (R2(x)-values are equal to 0 anyhow!) cannot be regarded as acceptable. The RO3(y)(3x3)-values are just around the limit of acceptance.

Figures 6-8 show the results if twin control is used instead of single control. The reliability of the non-control points is not much improved by this procedure (maximum improvement: 9% for RO3(y) in block 43). The reliability of the outer rays of the control points, however, improves significantly: 17% for CRO4/9(x,y) in blocks 43 and 73. A particular behavior is shown by the inner rays of the non-control and control points. Since their reliability is already very high in the case of single control there is practically no improvement involved by using twin control. The maximum possible average reliability level for non-control points seems to be reached by the inner ray values of the points with 4-9 rays in the 5x5 blocks of the

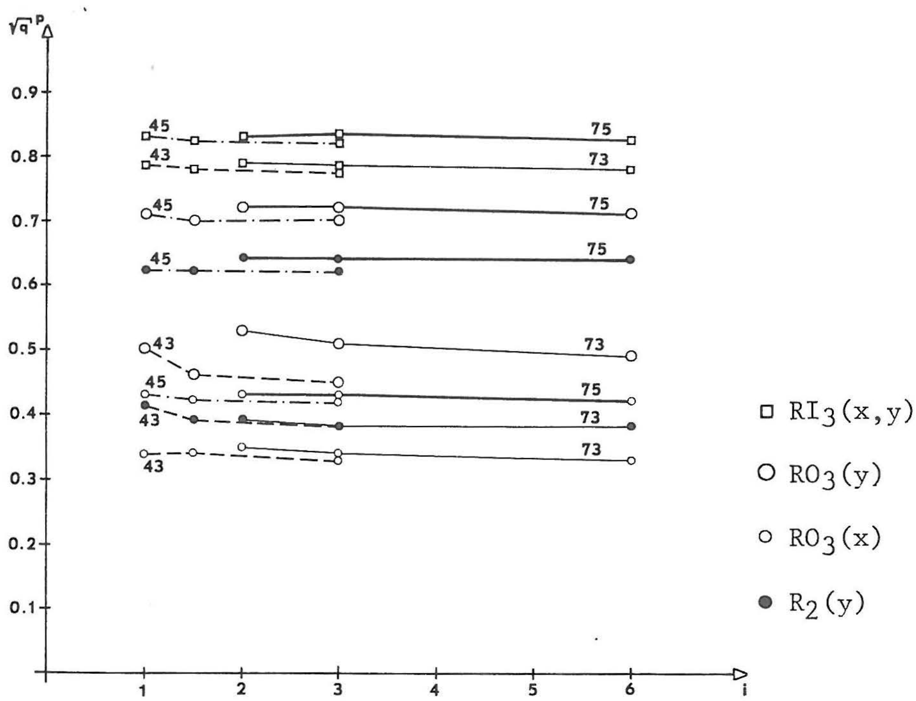

Figure 3: Point means $\sqrt{q}\,P$ for 2-ray and 3-ray non-control points

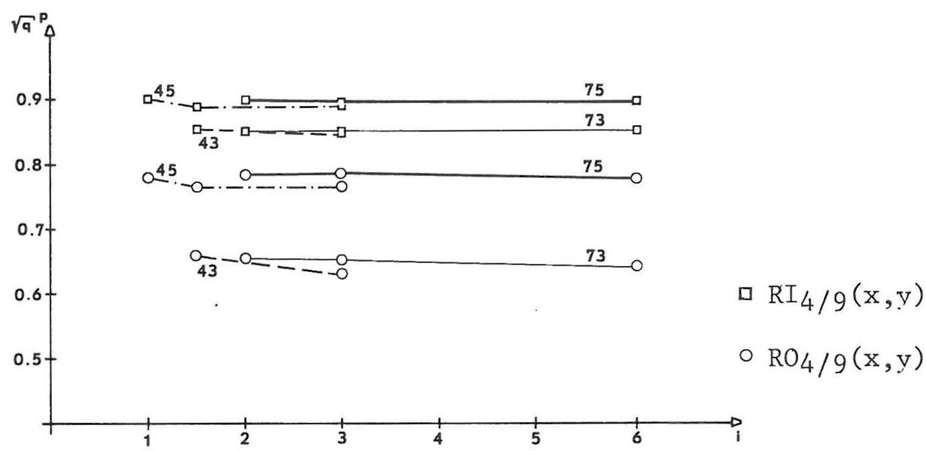

Figure 4: Point means $\sqrt{q}\,P$ for 4-9-ray non-control points

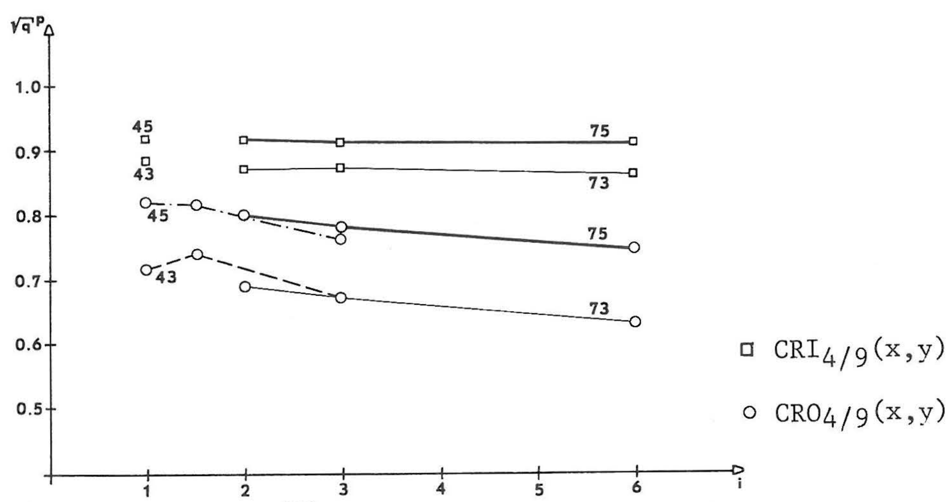

Figure 5: Point means $\sqrt{q}\,P$ for 4-9-ray control points

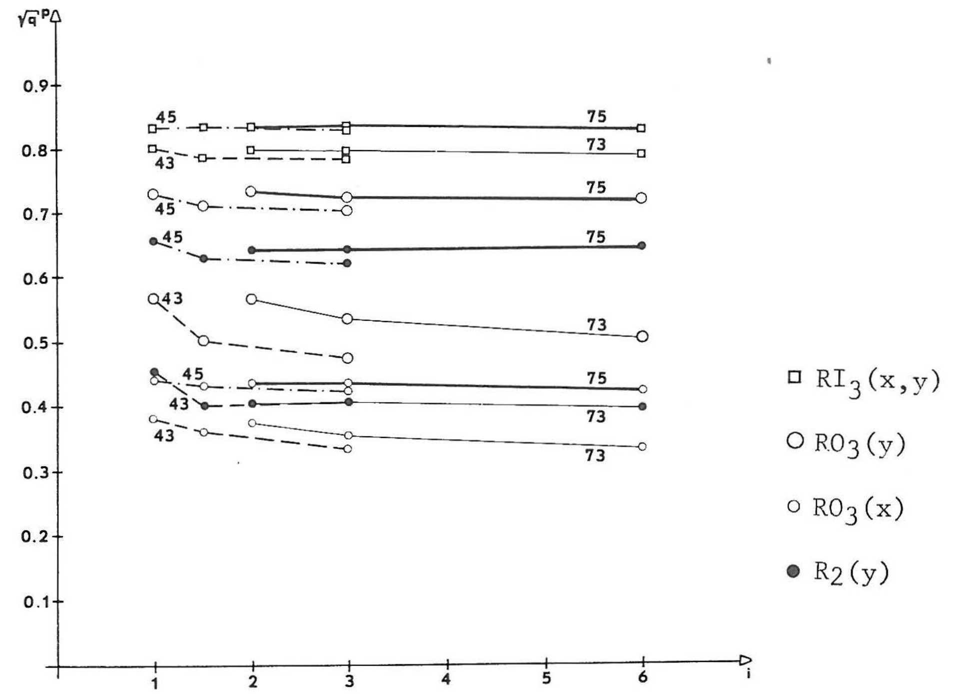

Figure 6: Point means $\sqrt{q}^p$ for 2-ray and 3-ray non-control points (twin control version)

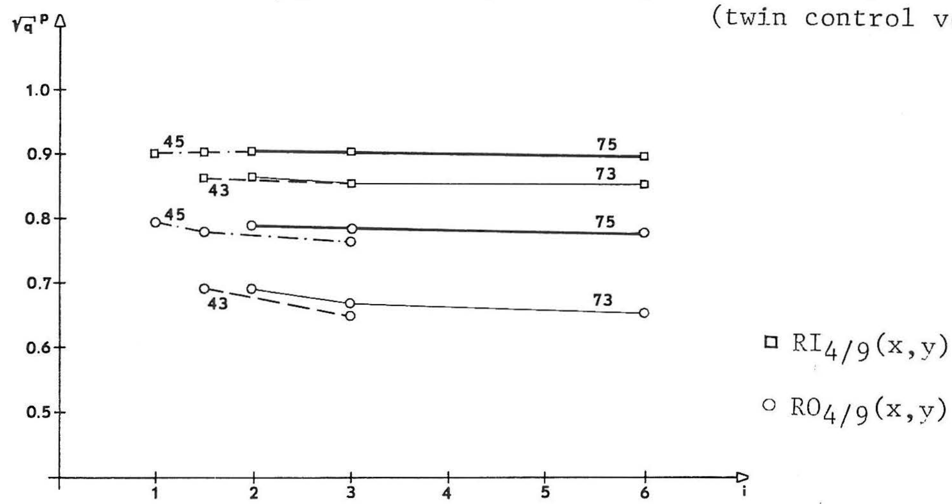

Figure 7: Point means $\sqrt{q}^p$ for 4-9-ray non-control points (twin control version)

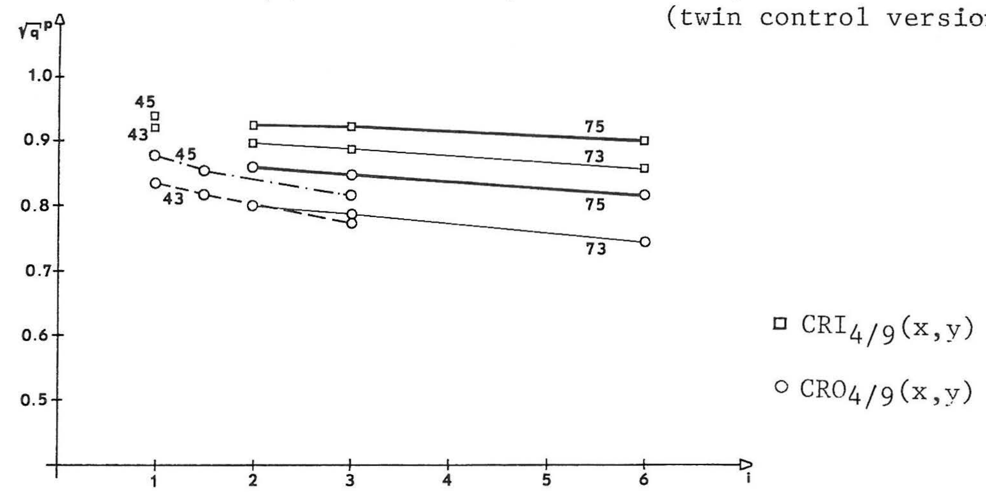

Figure 8: Point means $\sqrt{q}^p$ for 4-9-ray control points (twin control version)

twin control version (see Figure 7). The value of 0.90 remains unchanged, no matter which control bridging distance is used!
Although the dependence of the control point values on the bridging distance is only slight, this fact can be exploited by formulating the mean curves of Figures 5,8 analytically.
Then one obtains for a single control point:

$$\begin{array}{l} CRO_{4/9}(x,y) \begin{cases} 3x3 \\ 5x5 \end{cases} \\ CRI_{4/9}(x,y) \begin{cases} 3x3 \\ 5x5 \end{cases} \end{array} \sqrt{q_{vv}}p = \begin{cases} 0.735 - 0.018i \\ 0.825 - 0.013i \\ 0.885 - 0.004i \\ 0.920 - 0.002i \end{cases}$$

and for twin control:

$$\begin{array}{l} CRO_{4/9}(x,y) \begin{cases} 3x3 \\ 5x5 \end{cases} \\ CRI_{4/9}(x,y) \begin{cases} 3x3 \\ 5x5 \end{cases} \end{array} \sqrt{q_{vv}}p = \begin{cases} 0.835 - 0.015i \\ 0.870 - 0.008i \\ 0.920 - 0.010i \\ 0.940 - 0.007i \end{cases}$$

Replacing the curves of the different point classes of Figures 3-8 by average reliability numbers (ignoring also the slight dependence of the control values on the bridging distance), Table 2 is obtained. This Table shows very clearly the dependence of the average values on the number of image points per photo. Significantly better values are obtained with the 5x5 distribution, as far as outer ray observations are concerned. All inner ray observations and all control observations of the twin control versions are very resistant to a change in image point distribution. This behavior indicates the ways to improve the reliability of bundle networks.

Table 2: Average reliability values $\sqrt{q_{vv}}p$ for the observations of the different point classes

Point and observation classes	Block Means 43	73	45	75	Means for different image pt. distri. 3x3	5x5	Total Means
$R_2(y)$	0.40 *0.42*	0.38 *0.40*	0.62 *0.63*	0.64 *0.64*	★0.39 *0.41*	0.63★ *0.64*	---- ----
$RO_3(x)$	0.34 *0.36*	0.34 *0.37*	0.42 *0.43*	0.42 *0.43*	★0.34 *0.36*	0.42★ *0.43*	---- ----
$RO_3(y)$	0.47 *0.51*	0.51 *0.53*	0.70 *0.72*	0.72 *0.72*	★0.49 *0.52*	0.71★ *0.72*	---- ----
$RI_3(x,y)$	0.78 *0.79*	0.78 *0.79*	0.82 *0.83*	0.82 *0.83*	0.78 *0.79*	0.82 *0.83*	★0.80 *0.81*★
$RO_{4/9}(x,y)$	0.65 *0.69*	0.65 *0.67*	0.77 *0.78*	0.78 *0.78*	★0.65 *0.68*	0.78★ *0.78*	---- ----
$RI_{4/9}(x,y)$	0.85 *0.86*	0.85 *0.85*	0.90 *0.90*	0.90 *0.90*	0.85 *0.86*	0.90 *0.90*	★0.88 *0.88*★
$CRO_{4/9}(x,y)$	0.70 *0.81*	0.66 *0.78*	0.80 *0.85*	0.77 *0.84*	★0.68 *0.80*	0.78★ *0.84*	---- ★*0.82*★
$CRI_{4/9}(x,y)$	0.88 *0.92*	0.86 *0.89*	0.92 *0.94*	0.91 *0.92*	0.87 *0.90*	0.92 *0.93*	★0.89 *0.92*★

0.88...Single control results.
0.92...Twin control results.
★...Average values, recommended for use as approximate internal reliability values.

For the practical application of the modified data-snooping procedure it is crucial to investigate to what extent the average values derived from reliability models correspond to the strictly computed individual values. Due to lack of time this investigation could only be done with single control blocks. Here it was found out that with one exception all individual $\sqrt{q_{vv}}$-values remain within the ±25% tolerance range, if they are compared with the average values specially marked in Table 2. This exception concerns a part of the outer ray control observations $CRO_{4/9}(x,y)$ in all 3x3 image points blocks (see Figure 9).

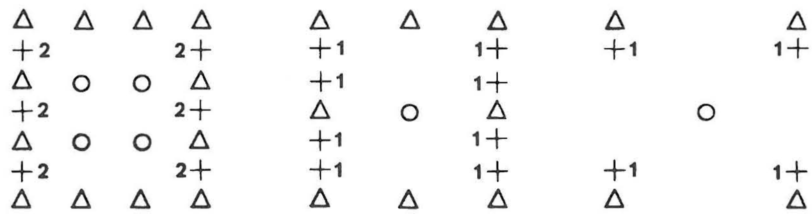

0.46 0.44 0.43

+2 ...2 outer ray control (y-) $\sqrt{q_{vv}}$-values of the photo in location + are smaller than 0.51 (0.51 = 0.68(1-0.25))

0.46...average $\sqrt{q_{vv}}$ - value of all these observations

Figure 9: Numbers of $CRO_{4/9}(y)$ - observations, which fall outside the tolerance limit given by ±25% (example: 73-blocks)

Here it is interesting to note that only that part of the y-observations, which belongs to perimeter photos, having only a half photo area coverage (6 image points), is concerned. This is an observation being made already in the previous investigations (Grün (2)). The reliability values of individual observations can be heavily reduced if these observations belong to photos which have a weak image point distribution, as it sometimes occurs in block perimeter photos. In this connection it is typical that no individual values of the 75-block observations exceed the tolerance limit, since the 5x5 image point distribution provides for better reliability especially for the perimeter photo observations.

4. Concluding remarks

The investigations presented in this paper are not complete in the sense that they do not cover all possible ray configurations. Geometric deviations from the regular patterns used here have also not been treated. As mentioned in the analysis of the results a weak image point distribution can lead to a considerable decrease of related reliability values, which should be taken care for in the applied blunder test procedure.
Internal reliability models have been derived which can serve different purposes. At first they show the weak parts of a photogrammetric bundle network. It is primarily the number of rays intersecting in a ground point and the general image point distribution which determines the internal reliability of a system, rather than the number and distribution of control points. Hence if good reliability is aspired for, two main aspects have to be considered. The flight arrangement should be planned in a way to obtain for each point to be assigned with coordinates at least fourfold photo coverage, i.e. 60% forward overlap and 60% sidelap or 20% sidelap crosswise flights. To get a sufficient image point distribution per photo

the perimeter photos should be stabilized, if necessary, by observing additional tie points and pass points.
As supplementary measures for the stabilization of the internal reliability the image coordinate observations should be performed in the stereomode and twin (or even multi) control points should be used. It is essential to state that stereomode observations do not only lead to better internal reliability but actually reduce the number of blunders considerably. To establish groups of control points requires not much more geodetic effort than is involved in the establishment of single control points. As additional benefit groups of control points provide for the insurance that if individual points get lost they easily can be recovered.
The second purpose that the internal reliability models can serve concerns the blunder detection procedure in practical blocks. In this paper a modified data-snooping procedure was suggested, requiring only a certain number of q_{vv}-values to be computed strictly. Considering the present uncertainty in the assumptions of the weights of the image coordinate observations it is even justifiable to eliminate the strict computations completely and to base the blunder detection procedure on the use of approximate $\sqrt{q_{vv}}$-values only.

References:

(1) Baarda, W.: A testing procedure for use in geodetic networks. Netherlands Geodetic Commission. Publications on Geodesy. Volume 2, Number 4, Delft 1967.

(2) Grün, A.: Gross error detection in bundle adjustment. Paper presented to the Symposium on Aerial Triangulation, Brisbane/Australia, Sept., 1979.

(3) Pope, A. J.: The statistics of residuals and the detection of outliers. Paper presented to the XVIth General Assembly of the IAG, Grenoble 1975.